The Enhanced Mechanical Properties of a Covalently Bound Chitosan-Multiwalled Carbon Nanotube Nanocomposite

Xiaodong Cao,[1,2] Hua Dong,[2] Chang Ming Li,[2] Lucian A. Lucia[1]

[1]*Department of Wood and Paper Science, North Carolina State University, Raleigh, North Carolina 27695-8005*
[2]*Division of Bioengineering, School of Chemical and Biomedical Engineering, Nanyang Technological University, Singapore 639798*

Received 16 July 2008; accepted 2 January 2009
DOI 10.1002/app.29984
Published online 19 March 2009 in Wiley InterScience (www.interscience.wiley.com).

ABSTRACT: In the present work, chitosan (CS)-grafted multiwalled carbon nanotube (MWCNT) nanocomposites were prepared via covalently bonded CS onto MWCNTs that had weight fractions of MWCNTs ranging from 0.1 to 3.0 wt % by a simple method of solution casting. The structure, morphology, and mechanical properties of the films were investigated by Fourier transform infrared spectroscopy, field emission scanning electron microscopy, optical microscopy, wide-angle X-ray diffraction, contact angle, and tensile testing. The results indicated that the CS chains were attached onto the MWCNTs successfully via covalent linkages. More interestingly, the MWCNTs provided a matrix that facilitated the crystallization of CS. Compared with the pure CS, the tensile strength and Young's modulus of the nanocomposites were enhanced significantly from 39.6 to 105.6 MPa and from 2.01 to 4.22 GPa with an increase in the MWCNT loading level from 0 to 3.0 wt %, respectively. The improvement in the tensile strength and modulus were ascribed to the uniform dispersion of MWCNTs covalently linked to the CS matrix.
 J Appl Polym Sci 113: 466–472, 2009

Key words: chitosan; multiwalled carbon nanotubes; nanocomposite; tensile strength

INTRODUCTION

Carbon nanotubes (CNTs) have been considered ideal reinforcing fillers for polymer matrices since their discovery in 1991 because of their nanometer size, high aspect ratios, and, more importantly, their excellent mechanical properties and high electrical and thermal conductivity.[1–3] These nanocomposites are usually developed to provide enhanced mechanical performance such as improved load transfer and tear resistance and to achieve certain levels of electric conductivity by providing a percolation network for charge migration and electromagnetic shielding.[4,5] It is well known that the physical properties of the nanocomposites mainly depend on the dispersion of fillers in the polymer matrices. However, CNTs are generally insoluble and severely aggregate because of intrinsic van der Walls attractions among the nanotubes, and their homogeneous dispersion in the desired polymer therefore presents a great hurdle.[6] To overcome this hurdle, various physical and chemical approaches have been previously considered, including the direct suspension of carbon nanotubes in the polymer solution via sonication,[7–12] *in situ* polymerization in the presence of CNTs,[13–16] and the chemical modification of CNTs to enhance solubilization.[17–21] Overall, the solubilization approach of CNTs via chemical functionalization is considered one of the most effective ways to achieve a homogeneous dispersion of CNTs in polymer matrices for high-quality nanocomposites. For example, it has been shown that by simply refluxing CNTs with nitric acid or mixed acids, the existing defects on the surface and ends of the CNTs that contain pendant hydroxyl groups can be preferentially oxidized by the acid to carboxylic groups. This thus greatly enhances the formation of nanocomposites with a great variety of polymer via covalent linkages. For example, it has already been shown that the carboxylic groups bound on CNTs can be used to attach aminopolymers via the formation of amide linkages.[22]

Another important approach to fabricate high-quality nanocomposites is through the proper selection of functionalities for chemical modification of the multiwalled carbon nanotube (MWCNTs). The most ideal and obvious way is to use a matrix polymer to provide functionality because it ensures compatibility of the dispersed CNTs with the matrix and avoids "impurities" associated with the dispersion agents and any potential microscopic phase separation in the nanocomposites. Sun and coworkers[15]

Correspondence to: X. Cao (xcao@ncsu.edu).

solubilized CNTs through the covalent attachment of polystyrene copolymers and then dispersed the polystyrene copolymer-functionalized CNTs into the polystyrene matrix for the fabrication of nanocomposite thin films. Hwang et al.[18] reported that the CNTs after grafting with poly(methyl methacrylate) (PMMA) could be well dispersed in a commercial grade of PMMA and significantly increase the storage modulus by 1300% for the amorphous PMMA containing 20 wt % of PMMA-grafted CNTs. Although much research on polymer-grafted CNTs nanocomposites has been performed, the matrices for these materials have mainly been synthetic-based polymers.[19,23] Reports of renewable and natural polymers as matrices for the MWCNTs have virtually been unseen in the literature.

Currently, the increasing cost of petroleum and the ever-increasing pollution from nondegraded synthetic polymers based on petroleum have directly threatened human beings' survival, health, and development. Therefore, biodegradable materials from renewable resources have attracted considerable attention for sustainable development and environmental preservation.[24] Chitosan, a copolymer of 2-amino-2-deoxy-β-D-gluocopyranose and 2-acetamido-2-deoxy-β-D-gluocopyranose, is the deacetylated derivative of chitin, one of the most plentiful natural polymers in the biosphere. Owing to its specific structure and properties, chitosan (CS) has attracted significant interest in a broad range of applications such as witnessed in biomedical, agricultural, and environmental fields.[25] However, the use of CT films has been largely restricted due to their inherent water sensitivity and relatively weak mechanical properties, especially in moist environments. An effective approach to cope with the issues of water sensitivity and inherently weak physical properties is to fabricate hybrid films that contain inorganic fillers, such as hydroxyapatite,[26] calcium phosphate cements,[27] and clay.[28] Although some successful CT-based nanocomposites have been reported, to our knowledge, most of them were obtained by noncovalent interactions such as blending,[11] layer-by-layer self-assembly,[29] surface deposition and crosslinking,[30] and electrochemical deposition on the surface of CNTs.[31]

In the present work, we first prepared the CS-grafted MWCNTs nanocomposites (CS-MWCNTs) via *in situ* covalent modification of MWCNTs with CT in the blending process at room temperature. The covalently modified MWCNTs are expected to be miscible with the CT matrix, allowing a relatively high amount of MWCNT incorporation without phase separation and leading to a significant enhancement of mechanical properties within the nanocomposite, which may broaden the applications of CT.

METHODS

Materials

Chitosan (medium molecular weight, 75–85% deacetylated) was purchased from Sigma-Aldrich (Singapore). It was dissolved in 2.0% aqueous acetic acid solution to give a polymer concentration of 1.0 wt % and then filtered and neutralized by 1*M* NaOH aqueous solution. The product was dried and used for all work. MWCNTs with a diameter of 10–20 nm and a length of 5–10 μm were purchased from Shenzhen Nanotech (Shenzhen, China). The MWCNTs were further refluxed in a mixture of concentrated sulfuric acid (98%) and nitric acid (60%) (v/v = 3 : 1) to produce more carboxylic acid groups.[32,33] After removing the supernatant by centrifugation, the remaining solid sample was washed repeatedly with deionized water until neutral. The solid sample was then vacuum dried. The coupling agents, 1-ethyl-3-(3-dimethyl aminopropyl) carbodiimide (EDC) and *N*-hydroxylsuccinimide (NHS), were purchased from Pierce (Rockford, IL) and Fluka (Sigma-Aldrich, Switzerland), respectively. The deionized water (18.2 MΩ cm) was produced from a Millipore Milli-Q water purification system (Millipore Corporation, Bedford, MA). All other reagents were analytical grade and used as received.

Preparation of the nanocomposite films

A stock solution of CS in aqueous acetic acid (1.0% by w/v) was prepared by dissolving 10 g CS in 1 L of aqueous acetic acid (1% by v/v). Grafting of CS on the MWCNT surfaces was conducted by using EDC and NHS as coupling agents, in which MWCNTs were dispersed in deionized water followed by reaction with a mixture of EDC and NHS (EDC/NHS = 1 : 2.5) for 2 h to activate the carboxylic acid groups on the MWCNTs. Subsequently, the desired amount of CS solution was added into the MWCNT dispersion with vigorous stirring. This reaction mixture yields an amide bond by activation of the carboxylic groups on surfaces of MWCNTs, followed by aminolysis of the *o*-isoacylurea intermediates by the amino groups of CS (Fig. 1). After 24 h of reaction at room temperature, the CS/MWCNT solution was degassed by sonication, followed by casting into a film. The cast film was dried in a vacuum oven at 60°C for 24 h. By changing the loading level of MWCNTs to 0.1, 0.3, 0.5, 0.8, 1.0, 2.0, and 3.0 wt %, a series of CS/MWCNT nanocomposite films was prepared and denoted as CS/MWCNTs-0.1, CS/MWCNTs-0.3, CS/MWCNTs-0.5, CS/MWCNTs-0.8, CS/MWCNTs-1.0, CS/MWCNTs-2.0, and CS/MWCNTs-3.0, respectively, in which the MWCNT loading level was expressed on water-free CS matrix. As a control, a CS film without MWCNTs was

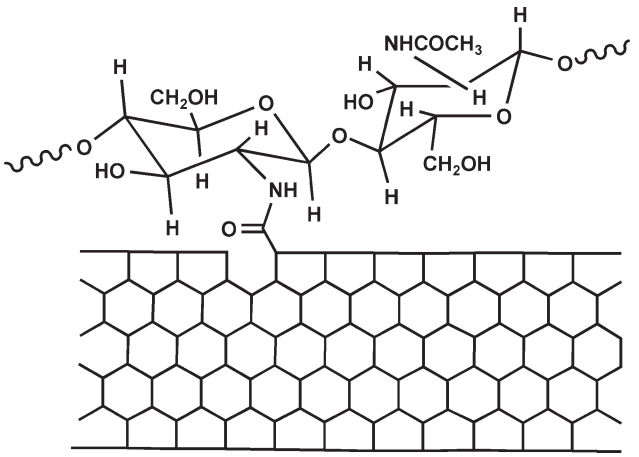

Figure 1 Schematic representation for the CS chain grafting onto the backbone of the MWCNTs.

obtained by using the same fabrication process. Before various characterizations, the resulting films were kept in a conditioning dessicator with 43% relative humidity for more than 1 week at room temperature to ensure the equilibration of the water in the films.

CHARACTERIZATION

FTIR was recorded on a Nicolet 5700 FTIR spectrometer (FTIR) (Thermo Electron, Waltham, MA) using KBr pellets. The data were collected from 4000 to 400 cm^{-1} employing 32 scans, which provided a resolution of 4 cm^{-1}.

The optical microscopy (OM) images of CS/MWCNTs nanocomposites were obtained by an Olympus IX71 inverted microscope (Center Valley, PA).

Scanning electron microscopy (SEM) measurements were carried out with field emission scanning electron microscopy (FESEM) (JEOL JSM-6700, JEOL, Tokyo, Japan). To evaluate the structure of the nanocomposites, the fracture surfaces of the CS/MWCNTs films after tensile testing were observed. The samples were coated with platinum and monitored with an accelerating voltage of 5 kV.

Wide-angle X-ray diffraction (WAXD) patterns were recorded on a Bruker AXS XRD station (Bruker AXS, Madison, WI), using Cu Kα radiation (λ = 0.154 nm) at 40 kV and 30 mA with a scan rate of 4°/min. The diffraction angle ranged from 4° to 40°.

The tensile strength and elongation at break of the films were measured on a universal testing machine (CMT 6503, Shenzhen SANS Test Machine, Shenzhen, China) at room temperature with a gauge length of 5 cm and crosshead speed of 10 mm/min. An average value of five replicates for each sample was taken.

Contact angle measurements of CS/MWCNTs nanocomposite films were executed by following the sessile drop method. A contact angle instrument equipped with an Image Analysis Attachment (First Ten Angstroms, Model FTA 100, Portsmouth, VA) was used. The probe liquid used in the experiments was deionized water. The water drop (2 μL) was carefully deposited on the surface of the nanocomposite film by using an assembled micrometer syringe. Because CS is a hydrophilic polymer, the contact angle measurement was recorded immediately after the water drop was deposited on the surface of the blend film. If the contact angle measurement was not immediately recorded after the water drop was deposited, the water drop became flat. Each reported data represent an average measured contact angle of at least five individual drops that were tested in different locations on the surface of a given film.

RESULTS AND DISCUSSION

Structure of the CS/MWCNTs nanocomposites

FTIR spectra of CS/MWCNTs and CS are shown in Figure 2. There are two characteristic absorbance bands centered at 1641 and 1566 cm^{-1} in the spectrum of CS, which correspond to the C=O

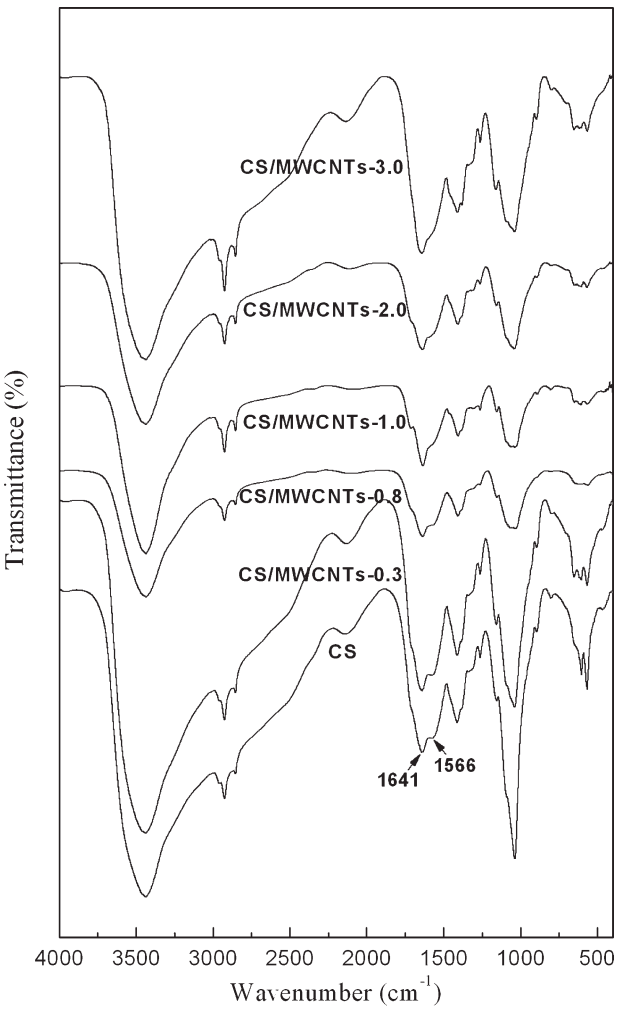

Figure 2 FTIR spectra of CS/MWCNTs and CS.

stretching vibration of —NHCO— (amide I) and the N—H bending of $—NH_2$, respectively. Compared to CS, a decrease in the intensity of $—NH_2$ absorbance band and an increase of the intensity of amide I can be easily observed in the spectra of the samples containing CS/MWCNTs that possess higher levels of MWCNTs loading level in the CS matrix. This result indicates that some $—NH_2$ groups on the CS chains have already reacted with the —COOH groups on the defect surfaces of the MWCNTs and therefore have been converted to —NHCO— groups. The grafting reaction also can be verified by observing their aqueous solution before casting. As shown in Figure 3, it can be seen that prior to the MWCNT grafting reactions, they precipitate. After the ensuing grafting reaction with CS in contrast, MWCNTs can be well dispersed in the CS aqueous solution for extended periods of time, which makes the casting method suitable.

The XRD patterns of the CS film, MWCNTs, and CS/MWCNTs nanocomposites with different loading level of MWCNTs, are shown in Figure 4, which in general serve to illustrate the influence of MWCNTs on the structure of the CS matrix. The ordering pattern of MWCNTs only exhibits a sharp reflection at about $2\theta = 25.8$, which is derived from the regular arrangement of the concentric cylinders of graphitic carbon.[34] However, this peak is absent in the patterns of CS/MWCNTs nanocomposites, indicating an effective dispersion of MWCNTs in CS.[35] The neat CS film shows characteristic peaks around $2\theta = 8.5°$, 11.3°, 18.3°, and 22.4°. The first two peaks correspond to the hydrated crystalline structure, whereas the broadened peak at about $2\theta = 22.4°$ indicates the existence of an amorphous structure.[36,37] It is worth noting that the intensity of the characteristic peaks of CS slightly increase with

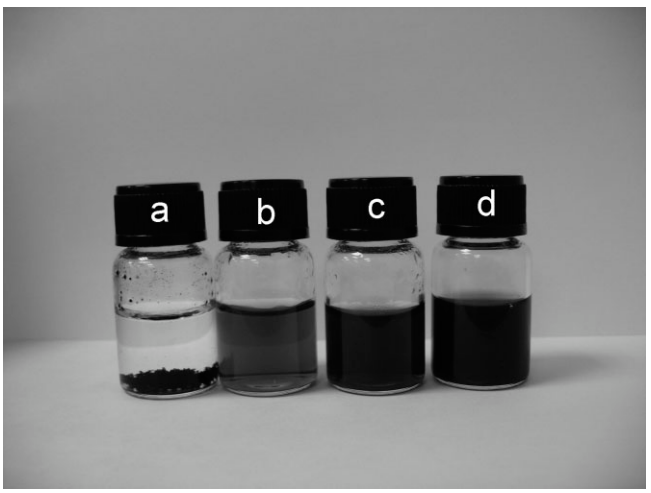

Figure 3 The appearance of samples in deionized water after 3 days: a, MWCNTs; b, CS/MWCNTs-0.3; c, CS/MWCNTs-1.0; d, CS/MWCNTs-3.0.

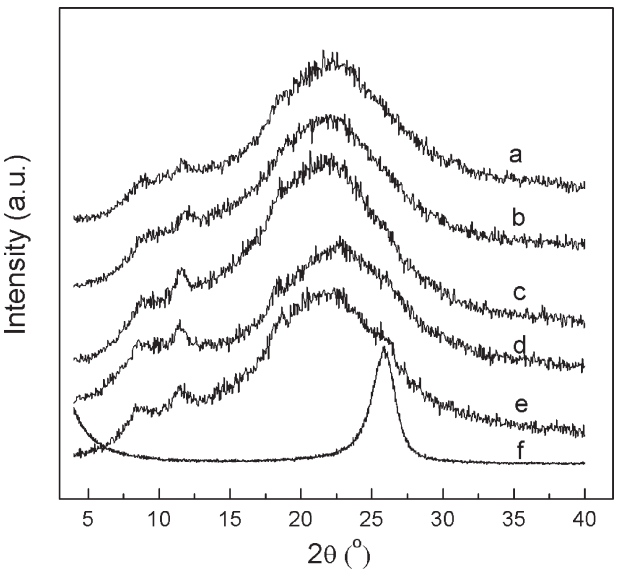

Figure 4 The WXRD patterns for CS/MWCNTs nanocomposites: a, CS; b, CS/MWCNTs-0.3; c, CS/MWCNTs-0.8; d, CS/MWCNTs-2.0; e, CS/MWCNTs-3.0; f, MWCNTs.

an increase in the concentration of MWCNTs in the CS matrix. A similar phenomenon also can be found in many other polymer-CNTs hybrids and is considered to be a result of polymer crystallization that is induced by CNTs.[38–40] In this particular case, after the reaction between CS and MWCNTs, the CS molecules are covalently attached to the surface of MWCNTs as supported by FTIR. The strong covalent bonding may contribute to a relatively ordered arrangement of the attached CS chains along the rigid template offered by MWCNTs.

Morphology of the CS/MWCNTs nanocomposites

The dispersion of MWCNTs in the CS matrix was detected by OM (Fig. 5). In contrast to the neat CS film, MWCNTs can be easily identified in these images. The MWCNTs appear as dark dots, the concentration of which on the surface of the nanocomposites film increases with an increase in their loading. There are no large aggregates observed, while a homogeneous distribution of the MWCNTs in the CS matrix can be observed in the nanocomposites when the loading level of MWCNTs is lower than 1.0 wt %, illustrating good adhesion between fillers and matrix. However, some larger black spots, which are attributed to MWCNTs aggregates, appear in CS/MWCNTs-2.0 and CS/MWCNTs-3.0.

Figure 6 illustrates the FESEM images of the fracture surfaces for CS and CS/MWCNTs nanocomposite films after tensile testing. In the SEM images no obvious large aggregates of MWCNTs were observed at the fracture surfaces for a MWCNT loading level lower than 1.0 wt %, suggesting that MWCNTs were dispersed homogenously in the

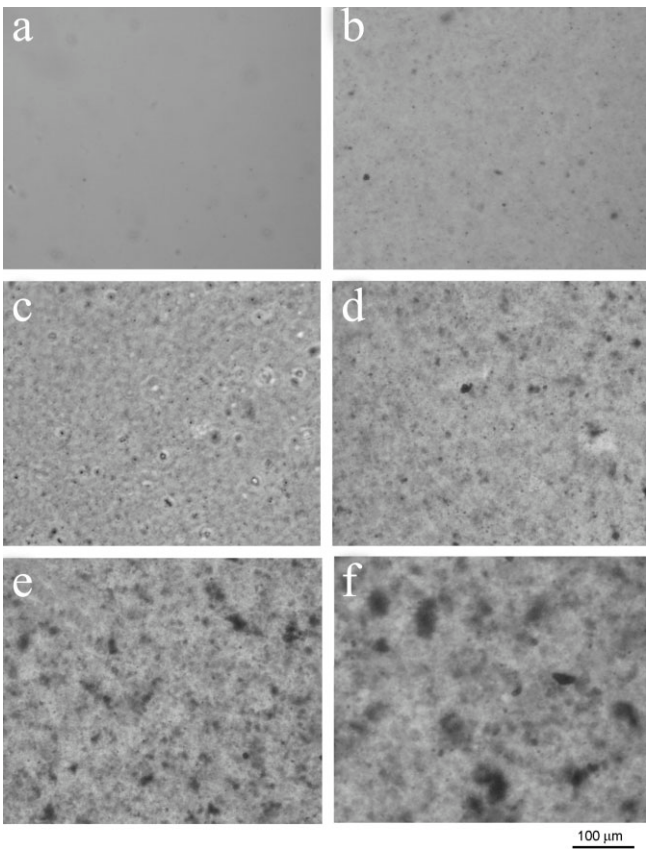

Figure 5 Optical microscopy images of CS/MWCNTs nanocomposite films containing different loading levels of MWCNTs: a, 0%; b, 0.3%; c, 0.8%; d, 1.0%; e, 2.0%; f, 3.0%.

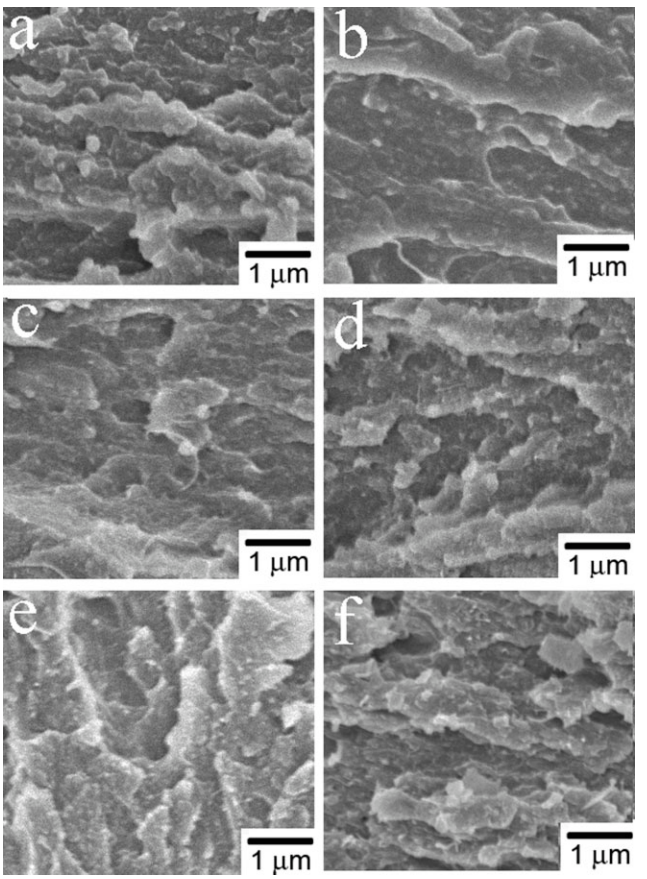

Figure 6 FESEM images of fractured surfaces in the CS/MWCNTs nanocomposites having different MWCNT loading levels: a, 0 wt %; b, 0.3 wt %; c, 0.8 wt %; d, 1.0 wt %; e, 2.0 wt %; f, 3.0 wt % (Scale bar: 1.0, 0.8 m).

CS matrix. However, with relatively higher MWCNT loading levels (2.0 and 3.0 wt %), a portion of the MWCNTs aggregate, while more exposed MWCNTs can be observed in the FESEM images of CS/MWCNTs-2.0 and CS/MWCNTs-3.0. Upon fracture, most of the MWCNTs are broken instead of being simply pulled out of the matrix. This observation definitively indicates that MWCNTs have good compatibility or linkage within the matrix. It has already been proven that chemical modification of MWCNTs in the matrix ensures the compatibility of the dispersed CNTs.[41] This latter phenomenon greatly contributes to avoiding the agglomeration of nonbound CNTS and thus any potential microscopic phase separation in the nanocomposites. An even and uniform distribution of the fillers in the matrix may play an important role in improvement of the mechanical performance of the resulting nanocomposite films.

Figure 7 demonstrates how the loading level of MWCNTs affects the initial contact angle values for the CS/MWCNTs nanocomposites at room temperature. The water contact angle of the neat CS film is $\sim 90^\circ$. It is noted that the contact angle on the nanocomosite films decreases very slightly when the MWCNT loading level increases from 0 to 1.0 wt %. This phenomenon can be attributed to the reduction in the exposed MWCNTs in the CS and hence the decrease in surface energy because most of the MWCNTs are completely bound in the CS matrix during the chemical modification. Yet, due to the

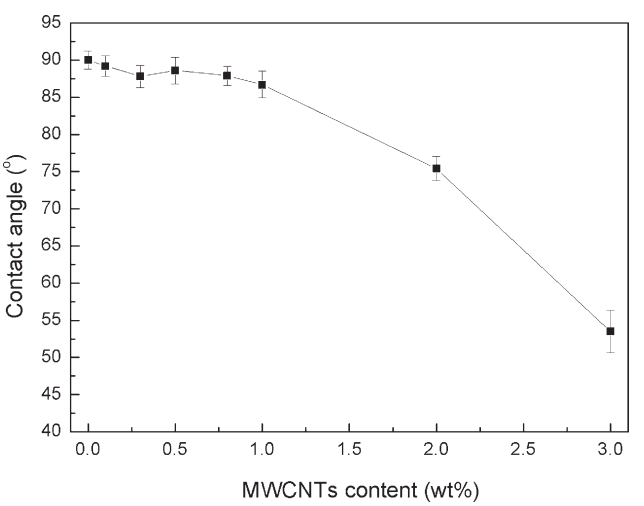

Figure 7 Dependence of the contact angle on MWCNTs' loading level for the CS/MWCNTs' nanocomposite films.

TABLE I
Mechanical Properties of the CS and CS/MWCNTs Nanocomposite Films Obtained from Tensile Testing

Samples	σ_b (MPa)	E (GPa)	ε_b (%)
CS	39.6 ± 3.2	2.01 ± 0.12	15.2 ± 1.2
CS/MWCNTs-0.1	50.6 ± 2.1	2.43 ± 0.23	14.1 ± 0.9
CS/MWCNTs-0.3	58.2 ± 4.6	2.65 ± 0.16	13.8 ± 1.3
CS/MWCNTs-0.5	76.3 ± 3.9	3.24 ± 0.23	13.3 ± 0.8
CS/MWCNTs-0.8	85.2 ± 6.8	3.52 ± 0.20	12.0 ± 0.5
CS/MWCNTs-1.0	98.3 ± 7.5	3.87 ± 0.25	11.3 ± 0.9
CS/MWCNTs-2.0	102.8 ± 3.6	4.35 ± 0.26	7.9 ± 1.1
CS/MWCNTs-3.0	105.6 ± 5.3	4.22 ± 0.14	5.6 ± 0.3

σ_b: tensile strength; E: Young's modulus; ε_b: elongation at break.

aggregation behavior of MWCNTs within the CS matrix at higher loadings of MWCNTs, the contact angle decreases dramatically. For instance, with 3 wt % of MWCNTs, the contact angle drops to a value of 53°.

Mechanical properties of the CS/MWCNTs nanocomposites

The mechanical behavior of the films of the plain CS matrix as well as the nanocomposites reinforced with various loading levels of MWCNTs were investigated by tensile tests at room temperature, and the corresponding data are presented in Table I. Clearly, the loading level of MWCNTs has a profound effect on the tensile properties. It is strongly evident that even a small amount of MWCNTs would significantly improve the tensile strength. The tensile strength and Young's modulus increased sharply from 39.6 to 105.6 MPa and from 2.01 to 4.22 GPa with an increase of MWCNTs loading level from 0 to 3.0 wt %, respectively. Furthermore, the gains in strength and modulus are obtained at a minimal expense in the elongation at break, which typically suffers much more in conventional filler–polymer systems as opposed to the current nanocomposite. More specifically, the elongation at break of the nanocomposite film of CS/MWCNTs-1.0 is 11.3%, which is a decrease of only 25.6% in comparison to that of the neat CS film, but, in contrast, the tensile strength and Young's modulus are 98.3 MPa and 3.87 GPa, dramatic increases of 148% and 92%, respectively. However, when the MWCNTs loading level is higher than 1.0 wt %, the tensile strength and Young's modulus increases slightly, but the elongation at break decreases from 11.3% to 5.6%. This may be attributed to a slight increase in the aggregation of the MWCNTs as verified by FESEM and OM. Generally, the results from the tensile tests indicate that the mechanical properties of the CS/MWCNTs nanocomposites are greatly improved in comparison to the neat CS. This can probably be explained by the reinforcement of the CS matrix by virtue of homogeneously dispersed MWCNTs fillers and the ensuing strong interaction between MWCNTs and the CS matrix. The MWCNTs are able to physically knot and tangle with the polymer chains of the CS matrix to achieve the reinforcement. Thus, MWCNTs act as network fulcrum points to transfer local stress evenly to all other CS chains, which in a general sense enhance the mechanical properties of the nanocomposites.

CONCLUSIONS

Biopolymer nanocomposites were prepared from CS as the matrix and acid-treated MWCNTs as reinforcing fillers by using EDC/NHS as coupling agents. The results of FTIR show that the CS chains are successfully linked to MWCNTs via reaction between the —NH_2 of CS and the —COOH of MWCNTs. The strong covalent linkages result in a relatively ordered arrangement of the CS chains containing the MWCNTs. The MWCNTs are dispersed in the CS matrix homogeneously as revealed by FESEM and OM, which dramatically enhance the mechanical properties of the nanocomposites. Compared with unfilled CS, the incorporation of only 1 wt % MWCNTs dramatically increases the tensile strength and Young's modulus by 148 and 92%, respectively, from 39.6 to 98.3 MPa and 2.01 to 3.87 GPa. Meanwhile, the elongation at break does not decrease significantly. The enhanced mechanical properties may therefore broaden the applications of CS in biochemical and electrochemical applications.

References

1. Iijima, S. Nature 1991, 354, 56.
2. Hughes, M.; Chen, G. Z.; Shaffer, M. S. P.; Fray, D. J.; Windle, A. H. Chem Mater 2002, 14, 1610.
3. Ajayan, P. M.; Stephan, O.; Colliex, C.; Trauth, D. Science 1994, 265, 1212.
4. Qu, L.; Lin, Y.; Hill, D. E.; Zhou, B.; Wang, W.; Sun, X.; Kitaygorodskiy, A.; Suarez, M.; Connell, J. W.; Allard, L. F.; Sun, Y.-P. Macromolecules 2004, 37, 6055.
5. Barrau, S.; Demont, P.; Peigney, A.; Laurent, C.; Lacabanne, C. Macromolecules 2003, 36, 5187.
6. Ruan, S. L.; Gao, P.; Yang, X. G.; Yu, T. X. Polymer 2003, 44, 5643.
7. Star, A.; Stoddart, J. F.; Diehl, M.; Boukai, A.; Wong, E. W.; Yang, X.; Chung, S. W.; Choi, H.; Heath, J. R. Angew Chem Int Ed 2001, 40, 1721.
8. Star, A.; Steuerman, D. W.; Heath, J. R.; Stoddar, J. F. Angew Chem Int Ed 2002, 41, 2508.
9. Qian, D.; Dickey, E. C.; Andrews, R.; Rantell, T. Appl Phys Lett 2000, 76, 2868.
10. Chen, J.; Liu, H.; Weimer, W. A.; Halls, M. D.; Waldeck, D. H.; Walker, G. C. J Am Chem Soc 2002, 124, 9034.
11. Wang, S.; Shen, L.; Zhang, W.; Tong, Y. Biomacromolecules 2005, 6, 3067.

12. Liu, T. X.; Phang, I. Y.; Shen, L.; Chow, S. Y.; Zhang, W. D. Macromolecules 2004, 37, 7214.
13. Barraza, H. J.; Pompeo, F.; O'Rear, E. A.; Resasco, D. E. Nano Lett 2002, 2, 797.
14. Shaffer, M. S. P.; Koziol, K. Chem Commun 2002, 2074.
15. Kumar, S.; Dang, T. D.; Arnold, F. E.; Bhattacharyya, A. R.; Min, B. G.; Zhang, X.; Vaia, R. A.; Park, C.; Adams, W. W.; Hauge, R. H.; Smalley, R. E.; Ramesh, S.; Willis, P. A. Macromolecules 2002, 35, 9039.
16. Qin, S.; Qin, D.; Ford, W. T.; Resasco, D. E.; Herrera, J. E. J Am Chem Soc 2004, 126, 170.
17. Ke, G.; Guan, W.; Tang, C.; Guan, W.; Zeng, D.; Deng, F. Biomacromolecules 2007, 8, 322.
18. Hwang, G. L.; Shieh, Y. T.; Hwang, K. C. Adv Funct Mater 2004, 14, 487.
19. Hill, D. E.; Lin, Y.; Rao, A. M.; Allard, L. F.; Sun, Y. P. Macromolecules 2002, 35, 9466.
20. Li, H. M.; Cheng, F. Y.; Duft, A. M.; Adronov, A. J Am Chem Soc 2005, 127, 14518.
21. Feng, W.; Bai, X. D.; Lian, Y. Q.; Liang, J.; Wang, X. G.; Yoshino, K. Carbon 2003, 41, 1551.
22. Riggs, J. E.; Guo, Z.; Carroll, D. L.; Sun, Y.-P. J Am Chem Soc 2000, 122, 5879.
23. Huang, W.; Lin, Y.; Taylor, S.; Gaillard, J.; Rao, A. M.; Sun, Y.-P. Nano Lett 2002, 2, 231.
24. Xu, Y. Y.; Gao, C.; Kong, H.; Yan, D. Y.; Jin, Y. Z.; Watts, P. C. P. Macromolecules 2004, 37, 8846.
25. Welsh, E. R.; Schauer, C. L.; Qadri, S. B.; Proce, P. R. Biomacromolecules 2002, 3, 1370.
26. Kim, S. B.; Kim, Y. J.; Yoon, T. L.; Park, S. A.; Cho, I. H.; Kim, E. J.; Kim, I. A.; Shin, J. W. Biomaterials 2004, 25, 5715.
27. Wang, J.; de Boer, J.; de Groot, K. J Dent Res 2004, 83, 296.
28. Darder, M.; Colilla, M.; Ruiz-Hitzky, E. Chem Mater 2003, 15, 3774.
29. Xu, Z. A.; Gao, N.; Chen, H. J.; Dong, S. J. Langmuir 2005, 21, 10808.
30. Liu, Y. Y.; Tang, J.; Chen, X. Q.; Xin, J. H. Carbon 2005, 43, 3178.
31. Luo, X. L.; Xu, J. J.; Wang, J. L.; Chen, H. Y. Chem Commun 2005, 2169.
32. Gao, C.; Vo, C. D.; Jin, Y. Z.; Li, W. W.; Armes, S. P. Macromolecules 2005, 38, 8634.
33. Liu, J.; Rinzler, A. G.; Dai, H. J.; Hafner, J. H.; Bradley, R. K.; Boul, P. J.; Lu, A.; Lverson, T.; Shelimov, K.; Huffiman, C. B.; Rodriguez-Macias, F.; Shon, Y. S.; Lee, T. R.; Colbert, D. T.; Smalley, R. E. Science 1998, 280, 1253.
34. Zhou, O.; Fleming, R. M.; Murphy, D. W.; Chen, C. H.; Haddon, R. C.; Ramirez, A. P. Science 1994, 263, 1744.
35. McNally, T.; Pötschke, P.; Halley, P.; Murphy, M.; Martin, D.; Bell, S. E. J.; Brennan, G. P.; Bein, D.; Lemoine, P.; Quinn, J. P. Polymer 2005, 46, 8222.
36. Jaworska, M.; Sakurai, K.; Gaudon, P.; Guibal, E. Polym Int 2003, 2, 198.
37. Rhim, J. W.; Hong, S. I.; Park, H. M.; Ng, P. K. J Agric Food Chem 2006, 54, 5814.
38. Grady, B. P.; Pompeo, F.; Shambaugh, R. L.; Resasco, D. E. J Phys Chem B 2002, 106, 5852.
39. Probst, O.; Moore, E. M.; Resasco, D. E.; Grady, B. P. Polymer 2004, 45, 4437.
40. Vladimir, E. Y.; Valentine, M. S.; Alexander, N. S.; Dmitriy, G. L.; Alexander, Y. F.; Gad, M. Macromol Rapid Commun 2005, 26, 885.
41. Lin, Y.; Zhou, B.; Shiral Fernando, K. A.; Liu, P.; Allard, L. F.; Sun, Y.-P. Macromolecules 2003, 36, 7199.